

## Article

# Estimation of the Chlorophyll-A Concentration of Algae Species Using Electrical Impedance Spectroscopy

Rinku Basak \*, Khan A. Wahid  and Anh Dinh

Department of Electrical and Computer Engineering, University of Saskatchewan, Saskatoon, SK S7N 5A9, Canada; khan.wahid@usask.ca (K.A.W.); anh.dinh@usask.ca (A.D.)

\* Correspondence: rib595@mail.usask.ca; Tel.: +1-306-203-6124

**Abstract:** Algae are a significant component of a biological monitoring program in an aquatic ecosystem. They are ideally suited for water quality assessments because of their nutrient requirements, rapid reproduction rate, and very short life cycle. Algae composition and temporal variation in abundances are important in determining the trophic level of lakes, and those can be estimated by the Chlorophyll-a (*Chl-a*) concentration of the species. In this work, a non-destructive method was employed to estimate the Chlorophyll-a concentration of multiple algae species using electrical impedance spectroscopy (EIS). The proposed EIS method is rapid, cheaper, and suitable for in situ measurements compared with the other available non-destructive methods, such as spectrophotometry and hyperspectral or multispectral imaging. The electrical impedances in different frequencies ranging from 1 to 100 kHz were observed using an impedance converter system. Significant observations were identified within 3.5 kHz for multiple algae species and therefore reported in the results. A positive correlation was found between the Chlorophyll-a and the measured impedance of algae species at different frequencies. Later, EIS models were developed for the species in 1–3.5 kHz. A correlation of 90% was found by employing a least squares method and multiple linear regression. The corresponding coefficients of determination were obtained as 0.9, 0.885, and 0.915, respectively for 49 samples of *Spirulina*, 41 samples of *Chlorella*, and 26 samples of mixed algae species. The models were later validated using a new and separate set of samples of algae species.

**Keywords:** electrical impedance spectroscopy; chlorophyll-a concentration; algae density; coefficient of determination



**Citation:** Basak, R.; Wahid, K.A.; Dinh, A. Estimation of the Chlorophyll-A Concentration of Algae Species Using Electrical Impedance Spectroscopy. *Water* **2021**, *13*, 1223. <https://doi.org/10.3390/w13091223>

Academic Editors: Shiming Ding and Qilin Wang

Received: 1 April 2021

Accepted: 26 April 2021

Published: 28 April 2021

**Publisher's Note:** MDPI stays neutral with regard to jurisdictional claims in published maps and institutional affiliations.



**Copyright:** © 2021 by the authors. Licensee MDPI, Basel, Switzerland. This article is an open access article distributed under the terms and conditions of the Creative Commons Attribution (CC BY) license (<https://creativecommons.org/licenses/by/4.0/>).

## 1. Introduction

Algae are a diverse group of aquatic organisms that can conduct photosynthesis. The algae species in water are classified with the colors or pigments. The *Arthrospira Platensis Spirulina* is a blue-green algae culture that is well-known as Cyanobacteria. *Spirulina* is 0.5 mm in length and rod- or disk-shaped. It is mostly found in mineral-rich alkaline lakes, rivers, and ponds. It is multicellular and the main photosynthetic pigment is phycocyanin, which makes it blue in color [1–3]. On the other hand, *Chlorella Vulgaris* is a genus of single-celled green algae belonging to the division Chlorophyta. It is mostly found in small polytrophic inland water bodies. It is spherical in shape, about 2–10 micrometers in diameter, and is without flagella [4–6].

*Spirulina* contains proteins (up to 70%), fatty or amino acids, minerals, vitamins (B<sub>12</sub>), antioxidant pigments, and Chlorophyll-a (*Chl-a*) [2,3,7]. *Spirulina* habitat with alkali water and require 27–32 degrees Celsius for growth. Nitrate is the main factor influencing both Chlorophyll and protein contents in *Spirulina* [3,7,8]. On the other hand, *Chlorella* contains green photosynthetic pigments, *Chl-a* and -b in its chloroplast, and small amounts of magnesium, zinc, copper, potassium, folic acid, and other B vitamins (1, 3, 8) [4,5]. *Chlorella* habitat with fresh water and require 25–27 degrees Celsius for growth [5,6,9].

Eutrophication is a very common phenomenon in dam reservoirs. It happens because of the enhancement of nutrients in the water. This has negative impacts on the water

quality of an aquatic system. The production of algae and aquatic plants is increased, and as a result algal blooms are formed [10]. *Chl-a* and transparency (Secchi depth) are the indicators of eutrophication and turbidity in aquatic ecosystems [10–13]. Prediction of these indicators helps us to know the trophic state of the reservoirs. The trophic levels can be managed efficiently by incorporating key environmental variables such as water temperature, nutrients, biological oxygen demand, and total suspended solids [13–15]. In addition, Secchi depth provides an estimate of the volume of the habitat of phytoplankton, which plays an important role in regulating the energy available to higher trophic level consumers in aquatic ecosystems. A rapid increase in phytoplankton biomass often results in nuisance algal blooms [16]. *Chl-a* is used as a proxy of phytoplankton biomass and is an important indicator in assessing the trophic status of freshwater ecosystems [11,12].

In addition, the nutritional components, such as carbon, nitrogen, phosphorus, and micronutrients, directly affect the algal growth, especially under high-density conditions [17–21]. Chlorophyll as a group of pigments is involved in all phototrophic organisms, including algae and some species of bacteria. The surface waters that show high *Chl-a* concentrations simultaneously contain high levels of nutrients, such as phosphorus and nitrogen. Therefore, *Chl-a* can be utilized as an indirect indicator of nutrient levels. *Chl-a* is the photosynthetic pigment that causes the green color in algae and plants [12,13]. Therefore, through the determination of *Chl-a* in water, the water quality status and the amount of algae in water can be known [14,15,22]. The overall algal biomass in a water body can be known by measuring *Chl-a*, which is extensively used as an indirect measurement. Thus, the existence of algae is indicated by *Chl-a* and turbidity, which in turn characterize the water quality [13,14,23]. The *Chl-a* concentrations are dependent upon many factors, such as water temperature, light level, nutrients, and the algal biomass and growth rate [13,24].

There are several direct and indirect methods of measuring *Chl-a* in water. In a direct method, dry weight measurements are usually performed after collecting water samples and the algal biomass is estimated [25,26]. Although the method is cost-effective, it is time consuming and destructive. On the other hand, optical characteristics of water samples are analyzed using different indirect and non-destructive lab-based methods such as spectrophotometry, fluorometry, high-pressure liquid chromatography (HPLC), and flow cytometry or hemocytometry (cell counting) [27–31]. Compared with fluorometry, spectrophotometry has a much higher detection limit (lower sensitivity). Spectrophotometry is widely used as an analytical method and preferable for monitoring microalgae culture systems [27,28]. A good estimation is also found using fluorometry, HPLC, and hemocytometry for water quality monitoring [29–31]. Although these methods have high accuracy, they are time consuming and require expensive instruments.

Previously, the *Chl-a* concentrations of algae species were determined using portable hyperspectral systems and multi-wavelength optical sensors with the help of several promising tools such as multiple linear regression (MLR), support vector machine (SVM), and artificial neural network (ANN) [22–24,32,33]. Principle Component Analysis (PCA) was utilized to reveal the relationship between *Chl-a* and its associated parameters [10]. Several portable sensors were utilized for remote sensing applications to estimate *Chl-a* using multispectral/hyperspectral imaging; however, those required extra circuitry for large data storage, which makes the system complex, heavier, and more expensive [34–36]. Although in situ measurements are possible using these imaging methods, they are not highly accurate like the other optical methods.

In recent years, electrical characteristics of algae species in water samples have been analyzed using impedance spectroscopy for different applications, such as monitoring microalgal cell health, the extraction of algae as a corrosion inhibitor, quantification of microalgal biomolecule content, and biosensing of algal toxins in water. The method of electrical impedance spectroscopy (EIS) was found to be non-destructive and suitable for algal research by the impedance measurement of a water sample. The electrochemical impedance of electrode material silica obtained from sea water diatom algae was studied using EIS [37]. Microalgal cell health was studied, and the corresponding phenotypes

were identified by measuring electrical impedance [38]. The electrical impedances of algae species were measured at different frequencies and the cell properties were studied. It was found that in a low-frequency range, cell size dominates the impedance. A large cell size exhibits a large impedance response at a lower frequency. The flow of current is obstructed when the cell size is closer to the dimensions of the sensing region, resulting in impedance changes on a large scale [38]. Hence, the current between two electrodes decreases and in turn the impedance increases. Extraction of Spirulina and red algae as a corrosion inhibitor of carbon steel was studied using impedance spectroscopy [39–41]. The properties of biomolecules in microalga cells were studied using a faster EIS method compared with conventional techniques. Algal toxin detection in water based on a biosensing technique using EIS was also studied [42,43]. The method was found to be suitable for repeatability and applicable for in situ measurements. A multichannel EIS analyzer was also considered for measuring the impedance of microfluidic cells and the proposed sensor was sensitive to differential measurements of small particles [44]. Hence, the EIS method can be used as an alternative to optical spectroscopy for water quality monitoring. Furthermore, the estimation performance can be potentially improved by considering multispectral impedance imaging using an electrical impedance tomography (EIT) system. An efficient multi-task structure for multi-frequency EIT and anomaly detection based on real and imaginary images was studied previously [45,46].

Furthermore, the EIS method has been widely applied in determining soil moisture content [47], plant nitrogen status [48,49], plant moisture content [50], and root biomass [51], in biological analysis [52], and in pH measurement [53]. Recently, EIS was used for the determination of leaf nitrogen concentrations and relative water contents for multiple crops [54,55]. The computation using EIS is complex, but it is model-dependent with high accuracy, and it works in a wide range of frequencies. The method of EIS is cost effective, fast, non-invasive, in situ, and makes possible on-board implementation and real-time monitoring compared with other non-destructive methods. The EIS sensor is less sensitive to environmental variables than other non-invasive tools. A suitable EIS sensor was chosen in this work for the impedance measurement of algae species in water samples with the target of determination of the amount of algae by estimating *Chl-a*, which is required for continuous assessment in water quality monitoring. The two most prominent algae species, Spirulina and Chlorella, are the sources of most of the nutrients in lakes. Hence, a method using an EIS sensor to estimate the *Chl-a* concentration of multiple algae species (Spirulina, Chlorella, and a mix of algae) is presented in this work.

## 2. Materials and Methods

### 2.1. Growing of Algae Species

In our study, we grew all algae species (Spirulina and Chlorella) in a controlled environment at room temperature (20 °C). The culture kits for the species were ordered from Algae Research Supply, CA, USA [56]. Each kit included a 50 mL volume culture flask with a breathable cap, 1 mL of dense culture inoculum equivalent to approx. 0.1 gm/L dry weight, f/2 nutrients with sodium nitrate (NaNO<sub>3</sub>) and sodium phosphate (NaPO<sub>4</sub>), and salts for growing algae species. The salts are a combination of sodium bicarbonate (NaHCO<sub>3</sub>), sodium chloride (NaCl), magnesium sulfate (MgSO<sub>4</sub>), and calcium chloride (CaCl<sub>2</sub>) and provide a needed carbon source for algae [20]. The experiment was carried out during June–August 2020. At first, a volume of 500 mL of culture media was prepared by adding salt and nutrients with half a liter of drinking water. The Spirulina were in higher pH media than the Chlorella. Algae species were grown in culture flasks by adding the culture inoculum with culture media. The stock solution was prepared by adding the culture media on different days of the growing stage of algae species. For the growing of algae, sunlight was used during the daytime, and at night a LED grow panel and a fluorescent light were used as light sources. A temperature of 25–32 degrees Celsius with external heating and a 16:8 light:dark condition were maintained [17–19]. Approximately

four weeks were required to grow the species, and the stock solution of algae culture was ready for further experiments.

## 2.2. Sample Preparation and Extracting Chlorophyll-a

The algae culture (stock solution) was diluted using the same water media and 15 mL samples of both algae species (*Spirulina* and *Chlorella*) with different densities (6.25–100%) were prepared as shown in Figure 1. Then, the stock solutions of both species were mixed in an equal ratio, and the stock was diluted to prepare 15 mL mixed algae samples of different densities. Different samples of high to low concentrations were prepared by varying the densities of the species. A total of 116 samples of the species were prepared (*Spirulina*, 49 samples; *Chlorella*, 41 samples; mixed algae, 26 samples). The amount of algae in the prepared samples was estimated by Secchi Disk Depth (*SDD*) measurements. The depth at which the disk is no longer visible is known as the Secchi depth and is related to water turbidity [12–15]. The *SDD* has been widely used to describe the variations in water properties, which are linked to the variations in algal biomass [12]. The *SDD* is still regularly used in lakes or reservoirs for the measurement of water clarity because the Secchi Disk is cheaper, portable, easier to use, and the results from model predictions are in good agreement compared with the other available tools [12–15,56,57]. It was found that the *SDD* index increases with the decrease in density of algae species. The Chlorophyll-a concentration of algae species is related to the *SDD* as follows:

$$\frac{1}{SDD} = k_w + k_c \text{Chl-a} \quad (1)$$

where  $k_w$  is the light attenuation of all components other than Chlorophyll-a, and  $k_c$  is the attenuation of light by Chlorophyll-a [12,58,59]. A modified relation was used to calculate the *Chl-a* concentration for all of the samples of algae species using [11,12] as follows:

$$\text{Chl-a} = e^{(2.997 - 1.47 \ln(SDD))} \quad (2)$$

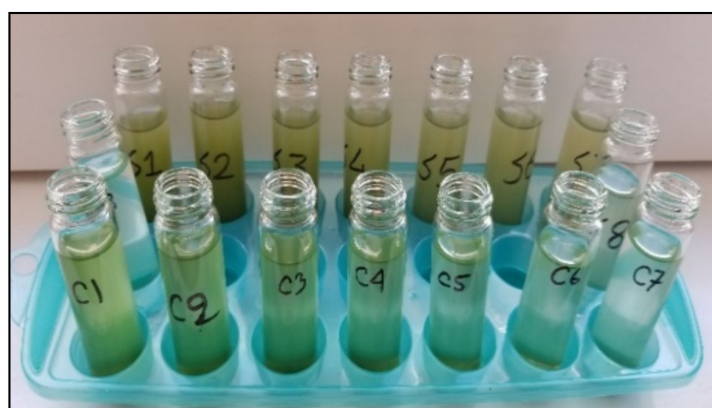


**Figure 1.** *Spirulina* and *Chlorella* samples at different densities (6.25–100%).

The *SDD* index for different concentrations of algae samples was recorded from 2.1 to 60.5 mm. The true *Chl-a* values of those were calculated as *Spirulina*, 1.65–114 mg/L; *Chlorella*, 1.24–12.2 mg/L; and mixed algae, 10.47–174 mg/L. The *Spirulina* samples were more highly concentrated than the *Chlorella* samples.

## 2.3. Experimental Setup

The electrical impedance spectroscopy (EIS) measurements of the algae samples were carried out using a portable impedance sensor (part # EVAL-AD5933EBZ) by varying the frequency from 1 to 3.5 kHz with 50 Hz intervals as shown in Figure 2. The EIS sensor used in the work has an accuracy of 0.5% and the sensor has a frequency sweep capability within

the frequency range of 1–100 kHz. Initially, the impedance profiles of the samples were observed over the whole frequency band up to 100 kHz, and we found an insignificant effect of the presence of salt, nutrients, and algae species in the water above 10 kHz. High impedance profiles and significant changes in impedance for different samples were observed within 3.5 kHz, and therefore considered for the models accordingly. In addition, it was found that the impedance of the samples decreased with an increase in the frequency.

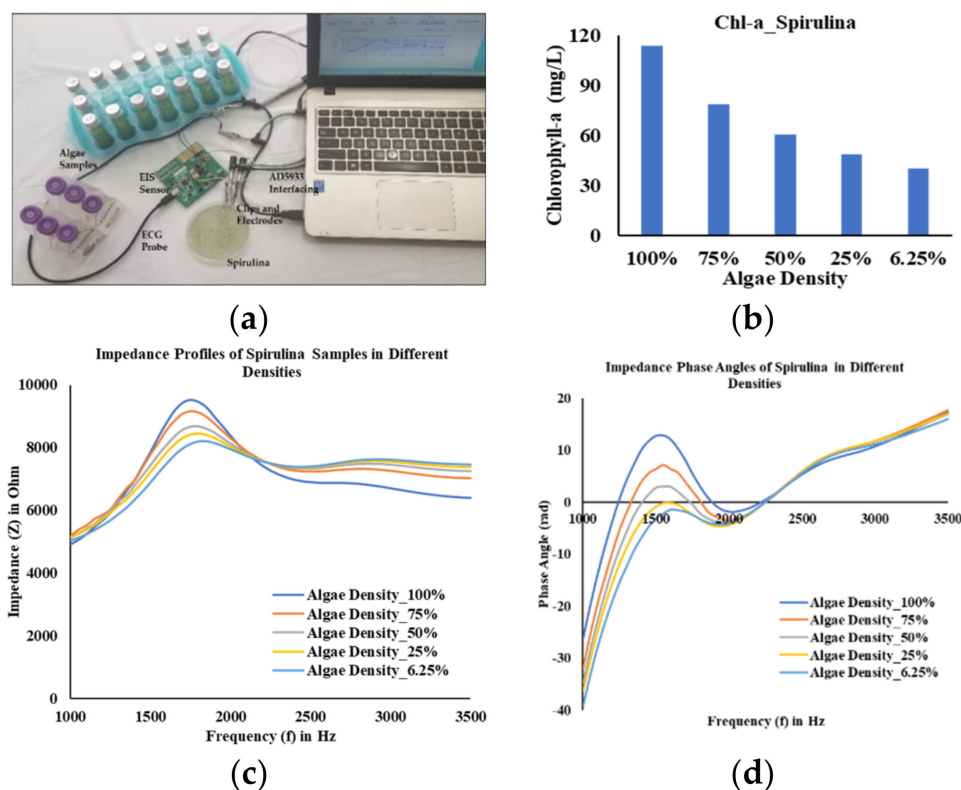


**Figure 2.** (a) EIS measurement setup for algae samples, (b) Chlorophyll-a for Spirulina samples, (c) the corresponding impedance profiles, and (d) the phase angles at different densities of Spirulina. The variation in algae density changes the impedance because of the different Chlorophyll-a concentrations of the species.

The experimental setup is presented in Figure 2a and the calculated Chlorophyll-a for different densities of Spirulina was recorded as shown in Figure 2b. At a lower density, the Chlorophyll-a of a sample was low because of the higher SDD and in turn the corresponding impedance was low as shown in Figure 2c. The impedance profiles were varied for different densities (6.25–100%) of Spirulina, and the corresponding phase angles are presented in Figure 2d. At a high density of algae species, the flow of current was obstructed, which caused the impedance to increase. A maximum impedance of 9.53 kOhm was obtained at 1.75 kHz for the algae density of 100% and with the decrease in density to 6.25% the corresponding maximum impedance was also decreased to 8.2 kOhm. The phase values were also decreased with the decrease in algae density.

The system voltage gain of AD5933 was calibrated with the output excitation voltage, feedback resistor, and programmable gain amplifier (PGA) gain. The gain through the system is given by

$$\text{Gain} = \text{Output Excitation Voltage} \times \frac{\text{Gain Setting Resistor}}{\text{Unknown Impedance (Z)}} \times \text{PGA Gain} \quad (3)$$

The sensor board has a flexible internal direct digital synthesizer (DDS) core and a digital-to-analog converter (DAC) that together generate the excitation signal used



to measure the unknown impedance ( $Z$ ). The output excitation voltage was  $0.2 \text{ V}_{\text{p-p}}$ . The small potential avoids the major current flow and maintains the technique as non-destructive. The  $PGA$  was set to times one ( $\times 1$ ) and according to [54,55] the impedance was obtained for different magnitudes by calibrating the analyzer gain factor with a known resistance of  $7.5 \text{ k}\Omega$  as:

$$\text{Impedance, } Z(\Omega) \propto \frac{1}{\text{Gain Factor}} \quad (4)$$

A high impedance of the sample was obtained for a low value of gain factor, which was adjusted by varying the frequency. The gain factor was obtained accordingly from  $1 \times 10^{-7}$  to  $9.9 \times 10^{-9}$ . In this work, we considered the magnitude of impedance only with the target of knowing the amount of algae in samples by the estimated Chlorophyll-a concentrations; phase was not taken into account. It is worth mentioning that the phase angle presents in detail the properties of biological matters, especially algal cell properties, cell strength, and cell size. However, only the magnitude of the impedance was used to develop the models, which reduced the computational complexity [45,60].

A pair of electrocardiogram (ECG) electrodes, connected to the sensor board with a separation of  $1 \text{ cm}$ , was used to measure the impedance of the algae samples non-invasively. At first, the distance between two electrodes was varied for the measurement of impedances at  $1\text{--}3.5 \text{ kHz}$ . For example, the impedance profiles of a *Chlorella* sample (C4) were obtained by varying the distance from  $0.6 \text{ cm}$  to  $1.25 \text{ cm}$  as shown in Figure 3. It was found that the overall impedance of the sample increased with the increase in separation of the electrodes. The capacitance between the two electrodes was decreased with the increase in distance and, hence, the impedance was increased with the increase in reactance. A good correlation was found at  $1 \text{ cm}$  for the measured impedances and, for this, all the measurements were taken in this work by keeping the separation of the electrodes at  $1 \text{ cm}$ . For the dipping electrodes, the effective area between electrode and solution was considered, which was varied by varying the length and diameter of the electrodes. The effective area was increased with the increase in either the effective length or the diameter of the electrodes. Hence, the capacitance was increased, resulting in the impedance of the sample being decreased [61]. By the subsequent experiments during the impedance measurements, the effective length of  $2 \text{ cm}$  and the diameter of  $0.03 \text{ inches}$  for the electrodes were chosen at the good correlation point.

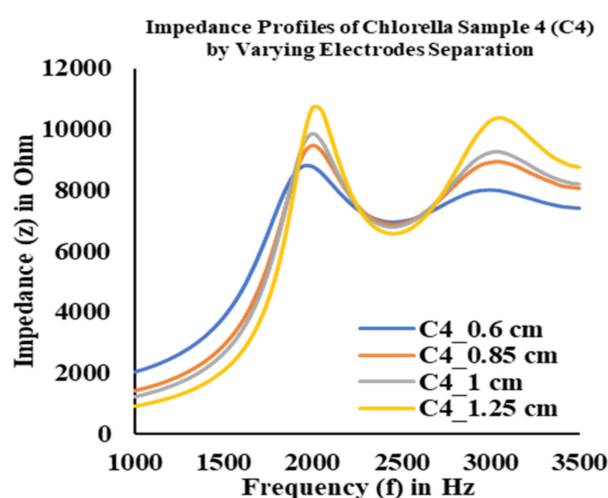


**Figure 3.** EIS measurements of a *Chlorella* sample (C4) by varying the distance between two electrodes from  $0.6$  to  $1.25 \text{ cm}$ . The impedance increases with the increase in the separation of the electrodes and the optimized distance was set to  $1 \text{ cm}$ .

The impedance at each frequency point was considered as a feature ( $k$ ). Therefore, a total of 51 features were selected for each sample considering frequencies of  $f_1, f_2$ , and  $f_{51}$ , respectively. A total of 49 samples ( $n$ ) of *Spirulina*, 41 samples ( $n$ ) of *Chlorella*, and 26 samples ( $n$ ) of mixed algae species were taken. For each sample, the measured dataset consisted of 51 impedance values; therefore, the datasets were taken as  $49 \times 51$ ,  $41 \times 51$ , and  $26 \times 51$ , respectively. At first, the impedances of different samples of the species along with the corresponding culture media were measured at 1–3.5 kHz considering negligibly small impedances of crocodile clip wires or electrodes. The impedance of the culture media was then subtracted from the measured readings of the samples to obtain the impedance of individual algae species and the effect of clips and electrodes was therefore eliminated. The dimensional dependencies of the electrodes and the corresponding effect on impedance for the sample under analysis were taken into account as discussed earlier. Any additional effect of the culture media components that can affect the algae impedance was cancelled out automatically. As a result, the actual impedance response of the algae species was obtained. It was then normalized to between 0 and 1 to avoid the negative values, if any. After normalization, the minimum and maximum values in the dataset were transformed into 0 and 1, respectively. A selectivity study was carried out to understand the effect of the presence of organic and inorganic matters in the impedance response. The chemical aspect between the water and the matters was also taken into account. The error was minimized by multiple measurements in a period for each sample in the controlled environment at room temperature and we maintained the measurement accuracy by checking the mean of those readings.

#### 2.4. Work Flow

A machine learning approach was utilized for the development of EIS models of multiple algae species. Multiple regression using the least squares method was employed with the help of PrimaXL ToolPak. The correlation ( $R$ ) between the normalized algae impedance ( $Z_n$ ) and the Chlorophyll-a concentration was determined using the XLMiner Analysis ToolPak. The regression models were obtained and validated by analysis of variance (ANOVA) T/F-tests. The coefficient of determination ( $R^2$ ), adjusted  $R^2$ , and root mean square error (rmse) were evaluated as performance parameters as follows:

$$R^2 = \frac{SSR}{SST} = \frac{\sum_{i=1}^n (\hat{y}_i - \bar{y})^2}{\sum_{i=1}^n (y_i - \bar{y})^2} \quad (5)$$

$$R^2_{adj} = 1 - \frac{SSR/(n-k-1)}{SST/(n-1)} = 1 - \frac{\sum_{i=1}^n (\hat{y}_i - \bar{y})^2 / (n-k-1)}{\sum_{i=1}^n (y_i - \bar{y})^2 / (n-1)} \quad (6)$$

$$rmse = \sqrt{\frac{SSE}{(n-k-1)}} = \sqrt{\frac{\sum_{i=1}^n (y_i - \hat{y}_i)^2}{(n-k-1)}} \quad (7)$$

where  $SSR$  is the sum of the square regression,  $SST$  is the sum of the square total,  $SSE$  is the sum of the square residual,  $y$  is the actual value,  $\hat{y}$  is the predicted value,  $\bar{y}$  is the mean of the actual value for  $n$  samples of algae species, and  $k$  is the number of features in a given frequency range [54,55].

Multi-collinearity among multiple features was examined for multiple regression. Most of the highly correlated features with a correlation of 95% or above, and the corresponding variance inflation factor (VIF) of 10 or above, were removed. The number of features in a dataset was selected accordingly using a wrapper backward elimination method. The importance of features were checked sequentially with the threshold probability of rejection of the null hypothesis  $p \leq 0.05$  using an individual T-test. The features with a large  $p$ -value (i.e., greater than 0.05) were removed and the features with  $p$ -values less than or equal to 0.05 were considered for the prediction. The null hypothesis states the exact opposite of what an experimenter predicts. It indicates strong evidence against the null hypothesis, as there is less than a 5% probability that the null hypothesis is correct.

Therefore, we reject the null hypothesis, and accept the alternative hypothesis. After a few iterations, the training and validations were performed using the least squares method considering the overall F-test ( $p \leq 0.05$ ), and the optimized multiple regression results were obtained for the algae species. The overall workflow of this work is presented in Figure 4. The predicted model of *Chlorophyll-a* using EIS was expressed with the help of multiple regression results for  $k$  features as follows:

$$\text{Chlorophyll-a} = \beta_0 + \beta_i Z_i, \text{ where, } i = 1, 2, 3 \dots k \quad (8)$$

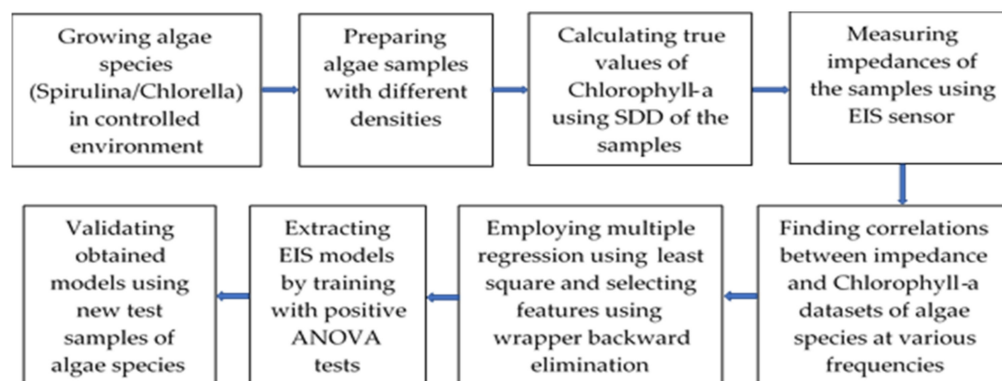


**Figure 4.** Workflow for the estimation of the Chlorophyll-a of multiple algae species using an EIS sensor system.

Here,  $\beta_0$  is the intercept and  $\beta_i$  is the coefficient for  $k$  features.

### 3. Model Development and Result Analysis

#### 3.1. Development of EIS Models

The impedances of *Spirulina* and *Chlorella* species for different samples were measured using an EIS sensor and those were correlated with the obtained Chlorophyll-a concentrations of the samples as shown in Figures 5 and 6, respectively. Overall, a positive correlation between impedance and Chlorophyll-a was found for both algae species at various frequencies. A high impedance was found for the high Chlorophyll-a concentration of *Spirulina* and the maximum impedance was obtained at 114 mg/L *Chl-a* at 1.7 kHz. When the concentration of Chlorophyll-a was decreased from 114 mg/L to 40.1 mg/L for five samples, the impedances also decreased accordingly as shown in Figure 5b. The correlation was 98% ( $R^2 = 0.96$ ) at 1.7 kHz as shown in Figure 5c. Multiple regression was employed at frequencies of 1–3.5 kHz for 49 samples of *Spirulina*, and 12 features were selected with positive ANOVA tests ( $p \leq 0.05$ ). The overall correlation was found to be 95% ( $R^2 = 0.9$ ) with an rmse of 7.7 mg/L and an adjusted  $R^2$  of 0.86 as shown in Figure 5d. On the other hand, the overall impedances for seven samples of *Chlorella* were decreased with the decrease in Chlorophyll-a from 6.37 mg/L to 1.84 mg/L as shown in Figure 6b. The correlation was obtained as 94.3% ( $R^2 = 0.89$ ) at 3.05 kHz as shown in Figure 6c. For the 41 samples of *Chlorella*, the overall correlation was 94% ( $R^2 = 0.885$ ) when employing multiple regression at frequencies of 1–3.5 kHz as shown in Figure 6d, 13 features were selected with positive ANOVA tests ( $p \leq 0.05$ ), and the obtained rmse and adjusted  $R^2$  were 1.13 mg/L and of 0.83, respectively.



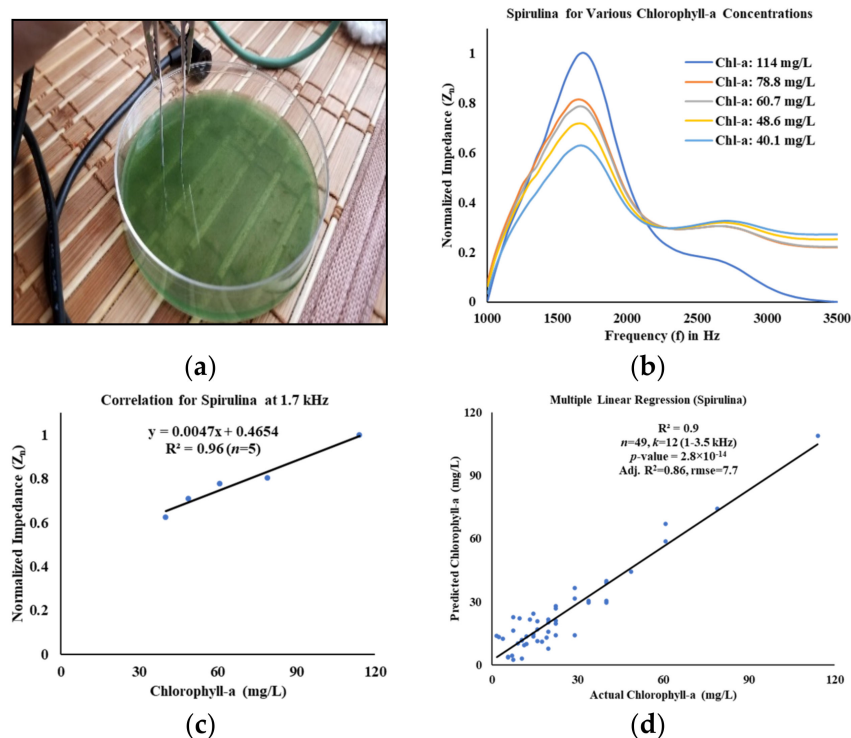


**Figure 5.** EIS measurements and performance analysis of Spirulina considering multiple regression: (a) measurement by the electrodes, (b) normalized impedance spectra, (c) correlation at 1.7 kHz, and (d) multiple regression at 1–3.5 kHz. Overall, a 95% correlation was found by the EIS measurements for 49 samples of Spirulina.

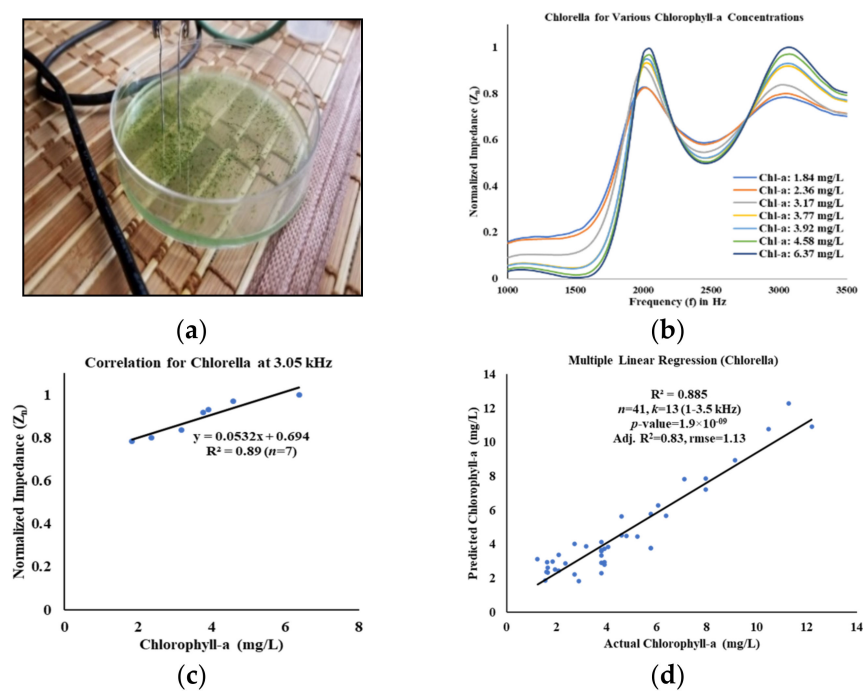


**Figure 6.** EIS measurements and performance analysis of Chlorella considering multiple regression: (a) measurement by the electrodes, (b) normalized impedance spectra, (c) correlation at 3.05 kHz, and (d) multiple regression at 1–3.5 kHz. Overall, a 94% correlation was found by the EIS measurements for 41 samples of Chlorella.

As a result, a good estimation of Chlorophyll-a was found and the corresponding EIS models for both *Spirulina* and *Chlorella* were extracted as given in Equations (9) and (10), respectively.

$$\begin{aligned} \text{Chlorophyll-a}(\text{Spirulina}) &= 293 - 3109Z_{n1.1 \text{ kHz}} + 3814Z_{n1.15 \text{ kHz}} - 1682Z_{n1.2 \text{ kHz}} \\ &+ 2779Z_{n1.55 \text{ kHz}} - 5205Z_{n1.85 \text{ kHz}} + 11674Z_{n2.4 \text{ kHz}} \\ &- 9466Z_{n2.6 \text{ kHz}} + 3827Z_{n2.9 \text{ kHz}} + 11923Z_{n3 \text{ kHz}} \\ &+ 27289Z_{n3.1 \text{ kHz}} - 35146Z_{n3.15 \text{ kHz}} - 7736Z_{n3.25 \text{ kHz}} \end{aligned} \quad (9)$$

$$\begin{aligned} \text{Chlorophyll-a}(\text{Chlorella}) &= 5.5 - 441Z_{n1.05 \text{ kHz}} + 1098Z_{n1.15 \text{ kHz}} - 550Z_{n1.2 \text{ kHz}} \\ &- 251Z_{n1.35 \text{ kHz}} + 510Z_{n1.45 \text{ kHz}} - 325Z_{n1.5 \text{ kHz}} + 413Z_{n1.9 \text{ kHz}} \\ &- 478Z_{n1.95 \text{ kHz}} + 119Z_{n2 \text{ kHz}} + 719Z_{n2.4 \text{ kHz}} - 677Z_{n2.45 \text{ kHz}} \\ &- 459Z_{n2.65 \text{ kHz}} + 322Z_{n2.85 \text{ kHz}} \end{aligned} \quad (10)$$

In another experiment, the sensor was tested by measuring the impedances of mixed algae species and the measurement data were correlated with the Chlorophyll-a values as shown in Figure 7. Multiple regression was employed and considered for the same frequencies of 1–3.5 kHz. The concentration of Chlorophyll-a was predicted for 26 samples of mixed algae species by selecting 15 features; the correlation achieved was 96% ( $R^2 = 0.915$ ) with positive ANOVA tests ( $p \leq 0.05$ ) for a rmse of 14.28 mg/L and an adjusted  $R^2$  of 0.79. The predicted EIS model for the estimation of the Chlorophyll-a of mixed algae species was extracted as given in Equation (11).

$$\begin{aligned} \text{Chlorophyll-a}(\text{mix algae}) &= -3249 + 2205Z_{n1.1 \text{ kHz}} - 2489Z_{n1.2 \text{ kHz}} + 2071Z_{n1.4 \text{ kHz}} \\ &+ 1341Z_{n1.45 \text{ kHz}} - 2507Z_{n1.5 \text{ kHz}} - 10098Z_{n2.25 \text{ kHz}} \\ &+ 13085Z_{n2.3 \text{ kHz}} - 2128Z_{n2.35 \text{ kHz}} - 9834Z_{n2.4 \text{ kHz}} \\ &+ 12348Z_{n2.45 \text{ kHz}} + 4326Z_{n2.55 \text{ kHz}} - 9267Z_{n2.7 \text{ kHz}} \\ &+ 42522Z_{n2.8 \text{ kHz}} - 26386Z_{n2.85 \text{ kHz}} - 10615Z_{n2.9 \text{ kHz}} \end{aligned} \quad (11)$$

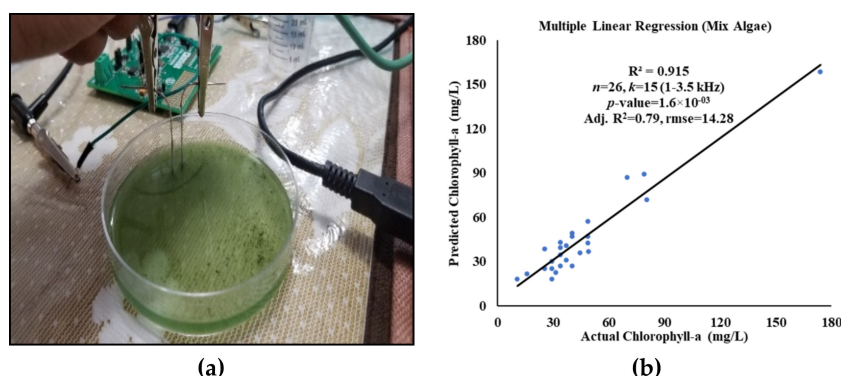


**Figure 7.** EIS measurements and performance analysis of mixed algae considering multiple regression: (a) measurement by the electrodes, and (b) multiple regression at 1–3.5 kHz. The overall correlation obtained was 96% for 26 samples of mixed algae species.

### 3.2. Validation of EIS Models

The extracted EIS models were validated by measuring the impedances for three new test samples of *Spirulina*, *Chlorella*, and mixed algae species. The true Chlorophyll-a concentrations of these three 15 mL samples of species were calculated using Equation (2) and the corresponding EIS measurements were carried out in the frequency range of 1–3.5 kHz. The culture media impedances were subtracted from the impedances of the samples and the corresponding impedances of three different algae species were obtained. The extracted

EIS models of Equations (9)–(11) of the species were fitted with the measured impedances at selected frequencies for the validation. The estimated Chlorophyll-a concentrations of the three different algae species found using the above EIS models were verified by comparing them with the true Chlorophyll-a values. The absolute error and the percentage accuracy were calculated and are shown in Table 1. The accuracy for Spirulina, Chlorella, and the mixed algae species was calculated as 85.7%, 84.4%, and 94.1%, respectively. The results show that the proposed EIS models performed well with high accuracy.

**Table 1.** Chlorophyll-a for the new test samples of algae species and validation of the EIS models.

Test Samples of Algae Species	True Chlorophyll-a Using Equation (2)	Estimated Chlorophyll-a Using EIS	Absolute Error =  True Value – Estimated Value	Percentage Accuracy
Spirulina	22.3 mg/L	25.5 mg/L	3.2 mg/L	85.7%
Chlorella	3.2 mg/L	3.7 mg/L	0.5 mg/L	84.4%
Mix Algae	61.5 mg/L	57.9 mg/L	3.6 mg/L	94.1%

### 3.3. Performance Evaluation of the Sensor

The performance of the EIS sensor was evaluated by the repeatability and sensitivity of the measurements. The measurements of the sensor were tested by taking the impedance readings of the same sample at least 10 times in half an hour in a controlled environment at room temperature. The accuracy of the measurements was found by obtaining similar readings and the mean of those was calculated as a final measurement, which reflected the repeatability of the EIS sensor. The impedances of algae species were measured, and the sensitivity of the sensor was calculated by the variation in Chlorophyll-a in the samples. The sensitivity is the slope of the output characteristic, which was measured at a particular frequency. A good sensitivity performance of the sensor was found for a wide range of Chlorophyll-a concentrations (1.24–174 mg/L) of the samples. At 1.7 kHz, the lowest sensitivity was calculated as 5.3 ohm per mg/L *Chl-a* (Figure 5c). A good prediction of Chlorophyll-a for different samples was found by the measured readings using the sensor and the error was checked by comparing them with the true values of those. The mean absolute error (MAE) for the extracted regression models of 49 samples of Spirulina, 41 samples of Chlorella, and 26 samples of mixed algae species was calculated as 5.23, 0.75, and 7.7 mg/L, respectively. Further, the error can be minimized by removing the anomalous data on the individual species.

The sensor was tested for distilled, spring, and tap water media and the electrical conductivity was studied with the variation in water salinity along with different matters in water. The presence of chemical and physical components in water may affect the sample impedance. The distilled water was mineral free and we found higher impedance because of the low number of electrolytes compared with the others. On the other hand, tap water and spring water contain a significant amount of minerals, resulting in a higher number of electrolytes. The natural spring water was found to be suitable for the growing of algae species and the algae culture was also diluted accordingly. A natural water system may contain several types of soluble, partially soluble, or insoluble matter along with algae species. An experiment of selectivity using the EIS sensor was conducted considering organic and inorganic matters in water. Beet powder, clay, spinach, and vinegar samples were taken along with algae based on the available minerals and Chlorophyll-a concentrations as shown in Figure 8. Algae of different sizes and colors may be present in lake water along with other soluble or insoluble matters. Spirulina contains a higher amount of minerals, such as calcium, potassium, and magnesium, than Chlorella and we found their impedance response at different frequencies. Other minerals, such as sodium, bicarbonate, phosphorus, and chloride, may also be present in the matters and the turbidity of the water sample may vary accordingly.

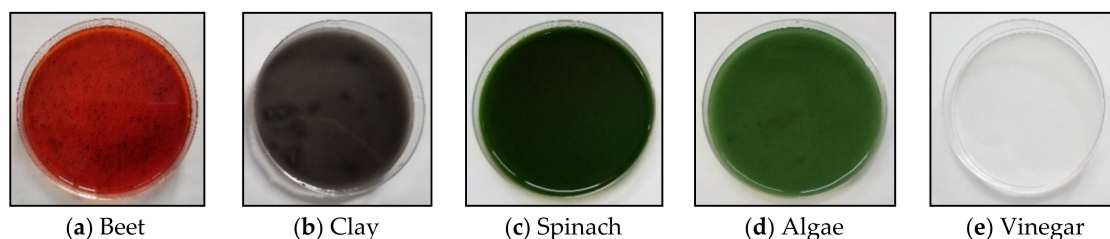


**Figure 8.** Samples of insoluble and soluble matters considered in the experiments: (a) beet powder, (b) clay, (c) spinach, (d) algae, and (e) vinegar, respectively.

The solubility and the corresponding electrolytes vary with respect to the available minerals, age, size, activity level, and water consumption of the matters. When the minerals dissolve in the water (partially or fully), they provide electrolytes with positive or negative ions, and the impedance of the corresponding sample can be found with the applied output excitation voltage. Among the selected matters, vinegar provides less electrolytes because it does not dissolve in water, but makes a homogenous solution. A high level of minerals is available in beet powder. Although it is not soluble in water, its red pigment is soluble. It is possible to have some red algae in water and, hence, the sample of beet powder was taken in the measurement. Clay is insoluble in water and its small particles absorb water slowly. Spinach provides a high number of electrolytes and is a very good source of Chlorophyll-a. Different turbid samples were prepared to resemble lake or river water samples.

The method of determination of a matter without any interference from other ingredients in a sample is called selectivity. The sensing of any molecular substances of the matter depends on the structure of the molecule and the temperature may affect the performance. The selectivity decreases with the increase in temperature. The molecular structure varies depending on the available minerals of soluble or insoluble matters. The selectivity was tested by measuring the impedances of the samples of different insoluble and soluble matters individually and comparing the readings with the measured impedance of the algae sample. Matters equivalent to 5 mg were added to the 15 mL of water media individually and the resulting impedances of all the samples were obtained as shown in Figure 9a. Spinach is soluble in water and three leaves were taken to prepare a sample. In addition, 5 mL of vinegar was taken in the measurements. The experiment was conducted at room temperature in a controlled environment. The response of the sensor was varied based on the selected matters in the samples. The sensor responded highly to the impedance response of the algae species (*Spirulina*) compared with the others. The corresponding phase values were also observed, and the samples were separated by the selective frequencies as shown in Figure 9b. The phase of the impedance changes because of the variation in the dimensions of the matters. The reactance varies, and in turn the impedance changes and responds to the different frequencies.

The clay particle was around 2  $\mu\text{m}$  in diameter, which is close to some lower-sized algae species and the sensor responded at 1.95 kHz for a sample. On the other hand, the beet powder particle had a larger diameter (approx. 3–4  $\mu\text{m}$ ) than the clay particle, which responded at 1.9 kHz. *Spirulina* is around 8  $\mu\text{m}$  in diameter and responded at 1.75 kHz. In addition, the response for the samples with higher and lower numbers of electrolytes, i.e., spinach and vinegar, was found at 1.85 kHz and 2 kHz, respectively. Thus, the impedance response may vary depending on the size of the available species in a sample and it was found that the response of the sensor for larger-sized particles in the sample shifts to the lower frequency [38]. The impedance response may also vary with the concentration of the species and was studied for all the individual matters accordingly. A frequency shift was observed because of the change in the reactance with the size and amount of the matters in water. The phase was also varied and shifted accordingly (Figure 9b). The flow of current was obstructed because of the larger cell size of algae species compared with the others and a high impedance was found as shown in Figure 9a. Even when the algae sample was diluted, the response was identified and discriminated from that of the other matters by

taking the exact concentration. As the other matters in a sample can be sensed by the EIS sensor (although it is not designed to do so), EIS is selective to algae (*Chl-a*) but not specific to it.

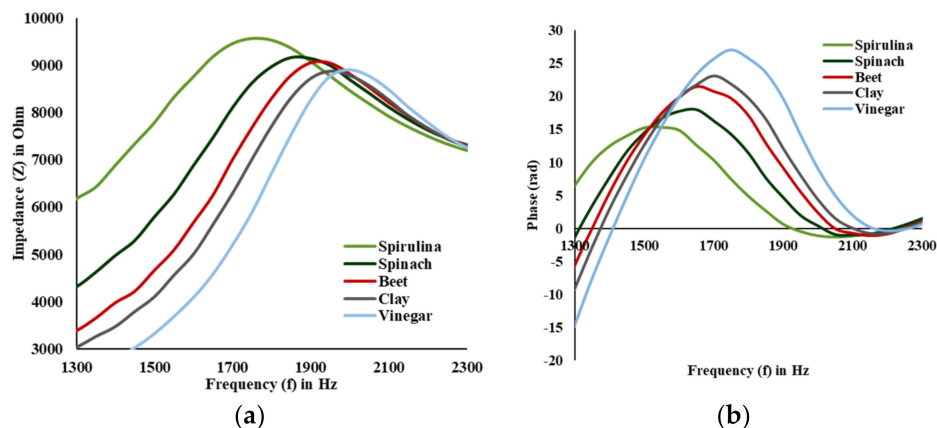


**Figure 9.** The EIS sensor's selectivity for the measurement of algae species in water: (a) the impedance response of the matters at different frequencies (Spirulina, 1.75 kHz; Spinach, 1.85 kHz; Beet, 1.9 kHz; Clay, 1.95 kHz; and Vinegar, 2 kHz), and (b) the corresponding phase of the impedance of the matters.

In addition, the robustness of the method was also tested as shown in Figure 10. Three different insoluble and soluble matters (beet powder, clay, and salt (NaCl) equivalent to 5 mg of the individual matters) were added to the 15 mL algae sample separately. A diluted algae sample and approximately similar matters to those in a lake sample were taken in the measurements. The impedances were measured before and after adding the matters to the algae sample as shown in Figure 10. A maximum impedance response of the algae sample was found at 1.8 kHz. No significant change in impedance was observed after adding the insoluble matters to the algae sample because of their smaller-sized particles compared with the algae species. The method was found to be selective as the sensor was able to measure the impedance of algae species for the given concentration in the presence of other ingredients in the sample. The addition of a high amount of matters may affect the performance on selectivity. On the other hand, the impedance of the algae sample decreased with the addition of NaCl (salt). Salt is soluble, and the conductivity increased in the mixed sample because of the higher number of electrolytes, which decreases the overall impedance. In addition, the response was shifted to 1.7 kHz. Overall, the method of using the EIS sensor was found to be robust and reliable for multiple unknown species.

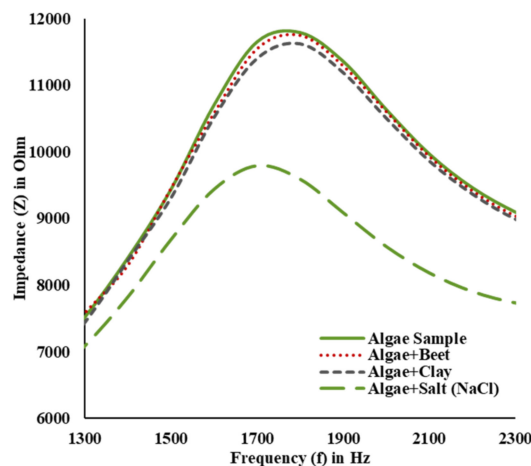


**Figure 10.** Robustness of the EIS sensor selectivity method in the presence of other ingredients in the sample.



#### 4. Discussion

A non-destructive EIS method was used to estimate the Chlorophyll-a concentrations of *Spirulina*, *Chlorella*, and mixed algae species at frequencies of 1–3.5 kHz. ANOVA tests were performed and EIS models were developed by selecting 12 features for *Spirulina*, 13 features for *Chlorella*, and 15 features for the mixed algae species. We considered the probability of rejection of the null hypothesis to be  $p \leq 0.05$  in T/F tests using the wrapper backward elimination method [54,55]. Overall, a positive correlation was found between algae impedance and Chlorophyll-a concentration at different frequencies.

The extracted Chlorophyll-a for different densities of the species indicated the presence and growth of algae [22,23,62]. Turbidity and trophic state are indicators used to monitor water quality in lakes or ponds [12]. Chlorophyll-a is a good candidate to study these two phenomena [12,13,15]. A high trophic state index (*TSI*) value of water indicates a high concentration of algae and poor lake water quality [12]. In addition, a high concentration of Chlorophyll-a indicates a high degree of turbidity and a high trophic state in a water body. The increase in biomass in a water body can be estimated using [11,12,58,59] with the calculation of *TSI* as:

$$TSI = 9.81 \ln(Chl-a) + 30.6 \quad (12)$$

Algae species dominate in a lake if the *TSI* ranges from 60 to 100 or above, and the corresponding water quality varies (fair or poor) based on the concentrations of algae species [12]. Highly concentrated algae samples were taken in this work, which indicated a high trophic state because of the high Chlorophyll-a concentration of 1.24 mg/L or above. A lake consisting of these values of *Chl-a* with a high *TSI* may be considered as having poor water quality in the class of hypereutrophic. Samples with a maximum *SDD* of 60.5 mm were taken in this work based on the available volume of stock solutions of grown algae species. The method using the EIS sensor can also be used to identify low concentrations of algae with Chlorophyll-a of less than 1.24 mg/L according to another study [61]. The rapid growth of algae can be identified by taking EIS measurements on a daily basis and the obtained data may help to develop warning indicators of algal blooms. *TSI* changes in a lake based on the suspended solids in the water body and the value decreases with the increase in the *SDD* [12]. *Chl-a* concentrations of algae can be extracted by obtaining the *SDD* from the surface to any depth of the lake. Usually, *Chl-a* is high near the top of the lake because the nutrient concentrations may be higher in this position than those deeper in the lake [12]. The over-enrichment of nutrients in water bodies may lead to an algal bloom because of a high amount of algae [12]. Moving towards the bottom of the lake, the *SDD* increases and the corresponding *Chl-a* concentration decreases because of the lower amount of algae species.

Several suspended solids, such as silt, sediment, bacteria, clay, and algae species, are available in the lake water. Algae species are photosynthetic organisms whose most important and major pigment is Chlorophyll-a that causes a green color in water [12,13,63]. The concentration of Chlorophyll-a present in the water is directly related to the amount of algae living in the water [12]. Hence, Chlorophyll-a is responsible mostly for the variation in impedance for different concentrations of algae species in water. A successful estimation of algae species was possible by this indirect measurement of Chlorophyll-a. The EIS method is model-dependent and reliable for the multiple algae species available in water. By obtaining the impedance spectrum and the peak intensities in a range of frequencies, a specific algae species can be identified. However, in this work, we considered pure and mixed cultures of two algae species (*Spirulina* and *Chlorella*) only. However, other algae species, such as diatoms and red algae species, may be available in lake water. From the measurements, a high impedance of *Spirulina* was found between 1 and 2 kHz (Figure 5b) and a high impedance of *Chlorella* was found between 2 and 3.5 kHz (Figure 6b). The cell size of *Spirulina* is larger than that of *Chlorella* and, hence, at a low frequency the flow of current was obstructed, and a high impedance of *Spirulina* was observed. The obtained results are in good agreement with the previous research [38]. The method of EIS

was found to be reliable because the models were tested and we found a good accuracy of higher than 84%. Other algae species can be studied in a similar manner.

A comparative study of EIS with the other methods for the estimation of *Chl-a* of algae species is presented in Table 2. It can be seen that the EIS technique is a good candidate and a cheaper (approx. \$150 USD) alternative to other available non-destructive methods.

**Table 2.** Comparative study of EIS with other non-destructive methods for the estimation of Chlorophyll-a in algae species.

	Excitation Source	Response	Detector	Cost	Operating Time	Accuracy (Affecting Factors)
Spectrophotometry [27,28]	LED/Laser (lower sensitivity)	absorbance	photodiode	expensive	approx. 2–3 min (lab)	accurate (optical distortion)
Fluorometry [29]	LED/Laser (higher sensitivity than spectro)	fluorescence	photodiode	more than spectro	approx. 5–6 min (lab)	more accurate than spectro
HPLC [30]	Laser (highly sensitive)	fluorescence	photodiode	highly expensive	approx. 15–20 min (lab)	highly accurate
Hemocytometry [31]	LED (sensitive to cell counts)	no. of cells	counting chamber	higher than EIS	approx. 5–10 min (lab)	accurate (miscounts large cells)
Multispectral Imaging [34–36]	LED (wavelength sensitivity)	reflectance	sensor probes	higher than EIS	approx. 1–2 min (in situ)	Accurate (data losses)
EIS (This Work)	voltage (frequency sensitivity)	impedance	electrodes	low cost	approx. 1 min (in situ)	Accurate (model-dependent)

## 5. Conclusions

In this work, a rapid, portable, and non-invasive method using electrical impedance spectroscopy (EIS) is proposed to estimate the Chlorophyll-a concentration of multiple algae species. The measurements were carried out at the end of the fourth week of the growth stage of all algae species, and a good correlation with Chlorophyll-a in the species was obtained by measuring the impedances in different frequencies ranging from 1 to 3.5 kHz. More than a 90% correlation with a high coefficient of determination (0.885 or above) was obtained considering multiple regression. The developed EIS models of the species were later validated using a new set of samples of *Spirulina*, *Chlorella*, and mixed algae species. The obtained accuracy for the models of the algae species ranges from 84% to 94%. Therefore, the proposed sensor performed well with high accuracy and offers itself as a useful candidate for water quality monitoring.

**Author Contributions:** R.B. performed the experiments and analyzed the data. R.B. and K.A.W. wrote the draft of the manuscript. K.A.W. and A.D. suggested for the experiments and data analysis, edited the draft. K.A.W. secured funding for this work. All authors have read and agreed to the published version of the manuscript.

**Funding:** This work is supported by the Canada First Research Excellence Fund (CFREF) through the Global Institute for Food Security (GIFS), University of Saskatchewan, Canada.

**Institutional Review Board Statement:** Not applicable.

**Informed Consent Statement:** Not applicable.

**Data Availability Statement:** Data is contained within the article.

**Acknowledgments:** The authors would like to extend their appreciation to Rakibul Islam Chowdhury, University of Saskatchewan, for his assistance during the experiment.

**Conflicts of Interest:** The authors declare no conflict of interest.

## References

1. Soni, R.A.; Sudhakar, K.; Rana, R.S. Spirulina—From growth to nutritional product: A review. *Trends Food Sci. Technol.* **2017**, *69*, 157–171. [\[CrossRef\]](#)
2. Ndjouondo, G.P.; Dibong, S.D.; Wamba, F.O.; Taffouo, V.D. Growth, Productivity and Some Physico-chemical Factors of Spirulina platensis Cultivation as Influenced by Nutrients Change. *Int. J. Bot.* **2017**, *13*, 67–74. [\[CrossRef\]](#)
3. Nuhu, A.A. Spirulina (Arthrospira): An Important Source of Nutritional and Medicinal Compounds. *J. Mar. Biol.* **2013**, *2013*, 1–8. [\[CrossRef\]](#)
4. He, L.; Chen, Y.; Wu, X.; Chen, S.; Liu, J.; Li, Q. Effect of Physical Factors on the Growth of Chlorella Vulgaris on Enriched Media Using the Methods of Orthogonal Analysis and Response Surface Methodology. *Water* **2020**, *12*, 34. [\[CrossRef\]](#)
5. Metsoviti, M.N.; Papapolymerou, G.; Karapanagiotidis, I.T.; Katsoulas, N. Effect of Light Intensity and Quality on Growth Rate and Composition of Chlorella vulgaris. *Plants* **2020**, *9*, 31. [\[CrossRef\]](#)
6. Enyidi, U.D. Chlorella vulgaris as Protein Source in the Diets of African Catfish Clarias gariepinus. *Fishes* **2017**, *2*, 1. [\[CrossRef\]](#)
7. Saeid, A.; Chojnacka, K.W. Evaluation of Growth Yield of Spirulina maxima in Photobioreactors. *Chem. Biochem. Eng. Q.* **2016**, *30*, 127–136. [\[CrossRef\]](#)
8. Barkallah, M.; Atitallah, A.B.; Hentati, F.; Dammak, M.; Hadrich, B.; Fendri, I.; Ayadi, M.A.; Michaud, P.; Abdelkaf, S. Effect of Spirulina platensis Biomass with High Polysaccharides Content on Quality Attributes of Common Carp (*Cyprinus carpio*) and Common Barbel (*Barbus barbus*) Fish Burgers. *Appl. Sci.* **2019**, *9*, 2197. [\[CrossRef\]](#)
9. Quintero-Dallos, V.; García-Martínez, J.B.; Contreras-Ropero, J.E.; Barajas-Solano, A.F. Crisostomo Barajas-Ferrerira, Roberto Lavecchia and Antonio Zuurro, Vinasse as a Sustainable Medium for the Production of Chlorella vulgaris UTEX 1803. *Water* **2019**, *11*, 1526. [\[CrossRef\]](#)
10. Chen, R.; Ju, M.; Chu, C.; Jing, W.; Wang, Y. Identification and Quantification of Physicochemical Parameters Influencing Chlorophyll-a Concentrations through Combined Principal Component Analysis and Factor Analysis: A Case Study of the Yuqiao Reservoir in China. *Sustainability* **2018**, *10*, 936. [\[CrossRef\]](#)
11. Carlson, R.E. A Trophic State Index for Lakes. *Limnol. Oceanogr.* **1977**, *22*, 361–369. [\[CrossRef\]](#)
12. Alemayehu, D.; Hackett, F. Water Quality and Trophic State of Kaw Lake. *J. Environ. Stud.* **2016**, *2*, 1–7.
13. Balali, S.; Hoseini, S.A.; Ghorbani, R.; Balali, S. Correlation of Chlorophyll-A with Secchi Disk Depth and Water Turbidity in the International Alma Gol Wetland, Iran. *World J. Fish. Mar. Sci.* **2012**, *4*, 504–508.
14. Lee, Z.P.; Shang, S.; Hu, C.; Du, K.; Weidemann, A.; Hou, W.; Lin, J.; Lin, G. Secchi disk depth: A new theory and mechanistic model for underwater visibility. *Remote Sens. Environ.* **2015**, *169*, 139–149. [\[CrossRef\]](#)
15. Liu, X.; Lee, Z.; Zhang, Y.; Lin, J.; Shi, K.; Zhou, Y.; Qin, B.; Sun, Z. Remote Sensing of Secchi Depth in Highly Turbid Lake Waters and Its Application with MERIS Data. *Remote Sens.* **2019**, *11*, 2226. [\[CrossRef\]](#)
16. Lee, S.; Lee, D. Improved Prediction of Harmful Algal Blooms in Four Major South Korea's Rivers Using Deep Learning Models. *Int. J. Environ. Res. Public Health* **2018**, *15*, 1322. [\[CrossRef\]](#)
17. Bawiec, A.; Garbowski, T.; Pawęska, K.; Pulikowski, K. Analysis of the Algae Growth Dynamics in the Hydroponic System with LEDs Nighttime Lighting Using the Laser Granulometry Method. *Water Air Soil Pollut.* **2019**, *230*, 1–11. [\[CrossRef\]](#)
18. Prates, D.F.; Radmann, E.M.; Duarte, J.H.; Morais, M.G.; Costa, J.A.V. Spirulina cultivated under different light emitting diodes: Enhanced cell growth and phycocyanin production. *Bioresour. Technol.* **2018**, *256*, 38–43. [\[CrossRef\]](#)
19. Fu, W.; Gudmundsson, O.; Feist, A.M.; Herjolfsson, G.; Brynjolfsson, S.; Palsson, B.Q. Maximizing biomass productivity and cell density of Chlorella vulgaris by using light-emitting diode-based photobioreactor. *J. Biotechnol.* **2012**, *161*, 242–249. [\[CrossRef\]](#) [\[PubMed\]](#)
20. Soni, R.A.; Sudhakar, K.; Rana, R.S. Comparative study on the growth performance of Spirulina platensis on modifying culture media. *Energy Rep.* **2019**, *5*, 327–336. [\[CrossRef\]](#)
21. Ak, I. Effect of an organic fertilizer on growth of blue-green alga Spirulina platensis. *Aquacult. Int.* **2012**, *20*, 413–422. [\[CrossRef\]](#)
22. Mamun, M.; Kim, J.J.; Alam, M.A.; An, K.G. Prediction of Algal Chlorophyll-a and Water Clarity in Monsoon-Region Reservoir Using Machine Learning Approaches. *Water* **2020**, *12*, 30. [\[CrossRef\]](#)
23. Keller, S.; Maier, P.M.; Riese, F.M.; Norra, S.; Holbach, A.; Börsig, N.; Wilhelms, A.; Moldaenke, C.; Zaake, A.; Hinz, S. Hyperspectral Data and Machine Learning for Estimating CDOM, Chlorophyll a, Diatoms, Green Algae and Turbidity. *Int. J. Environ. Res. Public Health* **2018**, *15*, 1881. [\[CrossRef\]](#)
24. Deng, J.; Chen, F.; Hu, W.; Lu, X.; Xu, B.; Hamilton, D.P. Variations in the Distribution of Chl-a and Simulation Using a Multiple Regression Model. *Int. J. Environ. Res. Public Health* **2019**, *16*, 4553. [\[CrossRef\]](#)
25. Delrue, F.; Alaux, E.; Moudjaoui, L.; Gagnard, C.; Fleury, G.; Perilhou, A.; Richaud, P.; Petitjean, M.; Sassi, J.F. Optimization of Arthrospira platensis (Spirulina) Growth: From Laboratory Scale to Pilot Scale. *Fermentation* **2017**, *3*, 59. [\[CrossRef\]](#)
26. Ross, M.E.; Stanley, M.S.; Day, J.G.; Semião, A.J.C. A comparison of methods for the non-destructive fresh weight determination of filamentous algae for growth rate analysis and dry weight estimation. *J. Appl. Phycol.* **2017**, *29*, 2925–2936. [\[CrossRef\]](#) [\[PubMed\]](#)
27. Agberien, A.V.; Örmeci, B. Monitoring of Cyanobacteria in Water Using Spectrophotometry and First Derivative of Absorbance. *Water* **2020**, *12*, 124. [\[CrossRef\]](#)
28. Rodrigues, L.H.R.; Arenzon, A.; Raya-Rodriguez, M.T.; Fontoura, N.F. Algal density assessed by spectrophotometry: A calibration curve for the unicellular algae Pseudokirchneriella subcapitata. *J. Environ. Chem. Ecotoxicol.* **2011**, *3*, 225–228.

29. Shin, Y.H.; Wing, M.T.G.; Choi, J.W. A field-deployable and handheld fluorometer for environmental water quality monitoring. *Micro Nano Syst. Lett.* **2018**, *6*, 1–6. [\[CrossRef\]](#)
30. Jones, J.; Manning, S.; Montoya, M.; Keller, K.; Poenie, M. Extraction of Algal Lipids and Their Analysis by HPLC and Mass Spectrometry. *J. Am. Oil Chem Soc.* **2012**, *89*, 1371–1381. [\[CrossRef\]](#)
31. Takahashi, T. Applicability of Automated Cell Counter with a Chlorophyll Detector in Routine Management of Microalgae. *Sci. Rep.* **2018**, *8*, 1–12. [\[CrossRef\]](#) [\[PubMed\]](#)
32. Ng, C.L.; Chen, Q.Q.; Chua, J.J.; Hemond, H.F. A Multi-Platform Optical Sensor for In Vivo and In Vitro Algae Classification. *Sensors* **2017**, *17*, 912. [\[CrossRef\]](#) [\[PubMed\]](#)
33. Jia, F.; Kacira, M.; Ogden, K.L. Multi-Wavelength Based Optical Density Sensor for Autonomous Monitoring of Microalgae. *Sensors* **2015**, *15*, 22234–22248. [\[CrossRef\]](#)
34. Cheng, C.; Wei, Y.; Lv, G.; Xu, N. Remote sensing estimation of chlorophyll-a concentration in Taihu Lake considering spatial and temporal variations. *Environ. Monit. Assess.* **2019**, *191*, 84. [\[CrossRef\]](#) [\[PubMed\]](#)
35. Baek, J.Y.; Jo, Y.H.; Kim, W.; Lee, J.S.; Jung, D.; Kim, D.W.; Nam, J. A New Algorithm to Estimate Chlorophyll-A Concentrations in Turbid Yellow Sea Water Using a Multispectral Sensor in a Low-Altitude Remote Sensing System. *Remote Sens.* **2019**, *11*, 2257. [\[CrossRef\]](#)
36. Wang, G.; Lee, Z.; Mouw, C. Multi-Spectral Remote Sensing of Phytoplankton Pigment Absorption Properties in Cyanobacteria Bloom Waters: A Regional Example in the Western Basin of Lake Erie. *Remote Sens.* **2017**, *9*, 1309. [\[CrossRef\]](#)
37. Nowak, A.P.; Lisowska-Oleksiak, A.; Wicikowska, B.; Gazda, M. Biosilica from sea water diatoms algae-electrochemical impedance spectroscopy study. *J. Solid State Electrochem.* **2017**, *21*, 2251–2258. [\[CrossRef\]](#)
38. Sui, J.; Fofonker, F.; Bhattacharya, D.; Javanmard, M. Electrical impedance as an indicator of microalgal cell health. *Sci. Rep.* **2020**, *10*, 1–9. [\[CrossRef\]](#)
39. Rodrigues, L.S.; Valle, A.F.; D’Elia, E. Biomass of Microalgae Spirulina Maxima as a Corrosion Inhibitor for 1020 Carbon Steel in Acidic Solution. *Int. J. Electrochem. Sci.* **2018**, *13*, 6169–6189. [\[CrossRef\]](#)
40. Mert, B.D.; Mert, M.E.; Kardas, G.; Yazici, B. The role of Spirulina platensis on corrosion behavior of carbon steel. *Mater. Chem. Phys.* **2011**, *130*, 697–701. [\[CrossRef\]](#)
41. Benabbouha, T.; Sinito, M.; Attari, H.E.; Chefira, K.; Chibi, F.; Nmila, R.; Rchid, H. Red Algae Halopitys Incurvus Extract as a Green Corrosion Inhibitor of Carbon Steel in Hydrochloric Acid. *J. Bio-Tribo-Corros.* **2018**, *4*, 1–9. [\[CrossRef\]](#)
42. Zhang, W.; Dixon, M.B.; Saint, C.; Teng, K.S.; Furumai, H. Electrochemical Biosensing of Algal Toxins in Water: The Current State-of-the-Art. *ACS Sens.* **2018**, *3*, 1233–1245. [\[CrossRef\]](#)
43. Zhang, W.; Jia, B.; Furumai, H. Fabrication of graphene film composite electrochemical biosensor as a pre-screening algal toxin detection tool in the event of water contamination. *Sci. Rep.* **2018**, *8*, 1–10. [\[CrossRef\]](#) [\[PubMed\]](#)
44. Ojarand, J.; Min, M.; Koel, A. Multichannel Electrical Impedance Spectroscopy Analyzer with Microfluidic Sensors. *Sensors* **2019**, *19*, 1891. [\[CrossRef\]](#)
45. Liu, S.; Huang, Y.; Wu, H.; Tan, C.; Jia, J. Efficient Multi-Task Structure-Aware Sparse Bayesian Learning for Frequency-Difference Electrical Impedance Tomography. *IEEE Trans. Ind. Inform.* **2021**, *17*, 463–472. [\[CrossRef\]](#)
46. Sapuan, I.; Yasin, M.; Ain, K.; Apsari, R. Anomaly Detection Using Electric Impedance Tomography Based on Real and Imaginary Images. *Sensors* **2020**, *20*, 1907. [\[CrossRef\]](#)
47. Umar, L.; Setiadi, R.N. Low cost soil sensor based on impedance spectroscopy for in-situ measurement. *Aip. Conf. Proc.* **2015**, *1656*, 040005.
48. Muñoz-Huerta, R.F.; Ortiz-Melendez, A.J.; Guevara-Gonzalez, R.G.; Torres-Pacheco, I.; Herrera-Ruiz, G.; Contreras-Medina, L.M.; Prado-Olivarez, J.; Ocampo-Velazquez, R.V. An analysis of electrical impedance measurements applied for plant N status estimation in lettuce (*Lactuca sativa*). *Sensors* **2014**, *14*, 11492–11503. [\[CrossRef\]](#)
49. Meiqing, L.; Jinyang, L.; Xinhua, W.; Wenjing, Z. Early diagnosis and monitoring of nitrogen nutrition stress in tomato leaves using electrical impedance spectroscopy. *Int. J. Agric. Biol. Eng.* **2017**, *10*, 194–205.
50. Kertész, A.; Hlaváčková, Z.; Vozáry, E.; Staroňová, L. Relationship between moisture content and electrical impedance of carrot slices during drying. *Int. Agrophys.* **2015**, *29*, 61–66. [\[CrossRef\]](#)
51. Postic, F.; Doussan, C. Benchmarking electrical methods for rapid estimation of root biomass. *Plant. Methods* **2016**, *12*, 1–11. [\[CrossRef\]](#) [\[PubMed\]](#)
52. Grossi, M.; Riccò, B. Electrical impedance spectroscopy (EIS) for biological analysis and food characterization: A review. *J. Sens. Sens. Syst.* **2017**, *6*, 303–325. [\[CrossRef\]](#)
53. Juansah, J.; Budiastara, I.W.; Dahlan, K.; Seminar, K.B. The prospect of electrical impedance spectroscopy as non-destructive evaluation of citrus fruits acidity. *IJETAE* **2012**, *2*, 58–64.
54. Basak, R.; Wahid, K.; Dinh, A. Determination of leaf nitrogen concentrations using electrical impedance spectroscopy in multiple crops. *Remote Sens.* **2020**, *12*, 566. [\[CrossRef\]](#)
55. Basak, R.; Wahid, K.A.; Dinh, A.; Soolanayakanahally, R.; Fotouhi, R.; Mehr, A.S. Rapid and Efficient Determination of Relative Water Contents of Crop Leaves Using Electrical Impedance Spectroscopy in Vegetative Growth Stage. *Remote Sens.* **2020**, *12*, 1753. [\[CrossRef\]](#)
56. Algae Research Supply. Available online: <https://algaeresearchsupply.com/pages/measuring-growth> (accessed on 21 October 2020).

- 
57. Brewin, R.J.W.; Brewin, T.J.; Phillips, J.; Rose, S.; Abdulaziz, A.; Wimmer, W.; Sathyendranath, S.; Platt, T. A Printable Device for Measuring Clarity and Colour in Lake and Nearshore Waters. *Sensors* **2019**, *19*, 936. [[CrossRef](#)]
  58. Quevedo-Castro, A.; Bandala, E.R.; Rangel-Peraza, J.G.; Amábilis-Sosa, L.E.; Sanhouse-García, A.; Bustos-Terrones, Y.A. Temporal and Spatial Study of Water Quality and Trophic Evaluation of a Large Tropical Reservoir. *Environments* **2019**, *6*, 61. [[CrossRef](#)]
  59. Sulis, A.; Buscarinu, P.; Soru, O.; Sechi, G.M. Trophic State and Toxic Cyanobacteria Density in Optimization Modeling of Multi-Reservoir Water Resource Systems. *Toxins* **2014**, *6*, 1366–1384. [[CrossRef](#)]
  60. Malone, E.; Santos, G.S.D.; Holder, D.; Arridge, S. Multifrequency Electrical Impedance Tomography Using Spectral Constraints. *IEEE Trans. Med Imaging* **2014**, *33*, 340–350. [[CrossRef](#)]
  61. Chowdhury, R.I.; Basak, R.; Wahid, K.A.; Nugent, K.; Baulch, H. A Rapid Approach to Measure Extracted Chlorophyll-a from Lettuce Leaves using Electrical Impedance Spectroscopy. *Water Air Soil Pollut.* **2021**, *232*, 1–12. [[CrossRef](#)]
  62. Michael, A.; Kyewalyanga, M.S.; Lugomela, C.V. Biomass and nutritive value of *Spirulina* (*Arthrospira fusiformis*) cultivated in a cost-effective medium. *Ann. Microbiol.* **2019**, *69*, 1387–1395. [[CrossRef](#)]
  63. Wang, Y.; Qu, T.; Zhao, X.; Tang, X.; Xiao, H.; Tang, X. A comparative study of the photosynthetic capacity in two green tide macroalgae using chlorophyll fluorescence. *SpringerPlus* **2016**, *5*, 1–12. [[CrossRef](#)] [[PubMed](#)]